BMC Pharmacology and Toxicology

RESEARCH Open Access

Melatonin enhances everolimus efficacy in breast cancer by suppressing mTOR pathway activation and promoting apoptosis and mitochondrial function

Şeyma Demirkesen[1], Yakup İriağaç[2], Erdoğan Selçuk Şeber[3] and Cenk Aral[1*]

Abstract

Background Everolimus is used in the treatment of breast cancer by targeting the PI3K/AKT/mTOR pathway, particularly during anti-hormonal therapy. The efficacy of everolimus is limited due to a feedback loop that supresses mTOR while simultaneously enhancing Akt activation in endocrine-resistant breast cancer. Melatonin (N-acetyl-5-methoxytryptamine) regulates mitochondrial activity, cell death, and autophagy due to its strong free radical scavenging, antioxidant, and anti-inflammatory characteristics. Melatonin, a naturally occurring oncostatic agent, slows tumor growth in a range of malignancies, including breast cancer. Due to its ability to protect healthy cells from oxidative stress and inflammation, along with its anti-cancer properties, melatonin has the potential to serve asan effective adjuvant in breast cancer therapy. It also inhibits the phosphorylation of mTOR and Akt, two essential pathways implicated in breast cancer growth, which may aid in overcoming resistance to targeted treatments like everolimus. The combination effects of melatonin and everolimus on hormone receptor-positive breast cancer remains unexplored. This study examined the effectiveness of melatonin when combined with everolimus for the treatment of hormone receptor-positive breast cancer.

Methods To investigate the effects of melatonin and everolimus combination, we divided MCF-7 cells into four experimental groups: the control, Melatonin (3 mM), Everolimus (30 nM), and a combination of Melatonin and Everolimus (3 mM + 30 nM). Cell viability, apoptosis, autophagy activation, and mitochondrial function were evaluated using established techniques.

Results Based on the cell viability test, the combination of 30 nM everolimus and 3 mM melatonin inhibited phosphorylation of 4E-BP1 and p70S6K, which are downstream effectors of the mTOR pathway, and reduced cell growth. In addition, co-administration of melatonin and everolimus increased apoptosis and led to Sub-G1 phase accumulation. LC3 protein expression and LC3 puncta analysis demonstrated autophagic activity. In terms of mitochondrial function, co-administration of melatonin with everolimus did not cause proton leakage or mitochondrial uncoupling, but did restore everolimus-induced respiratory inhibition.

*Correspondence:
Cenk Aral
caral@nku.edu.tr

Full list of author information is available at the end of the article

Conclusions In conclusion, melatonin is thought to improve the effectiveness of everolimus by inhibiting mTOR downstream effectors, enhancing apoptosis, activating autophagy, improving mitochondrial respiration, and reducing MCF-7 growth.

Graphical Abstract

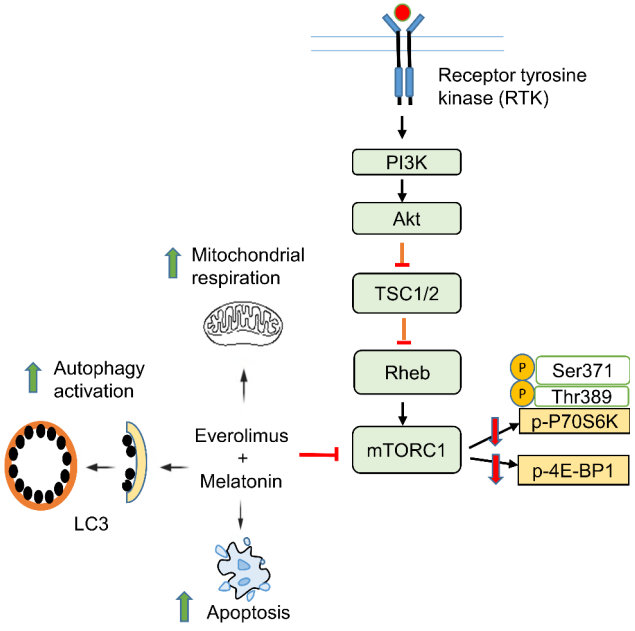

Keywords Melatonin, Everolimus, mTOR, Apoptosis, Autophagy, Mitochondrial respiration

Introduction

Despite medical breakthroughs, breast cancer remains the major cause of mortality among women. Two-thirds of all breast cancers express hormone receptors (ER+, HER2-) and rely on hormonal activation of several pathways for tumor cell survival and proliferation [1]. Although several therapeutic drugs that suppress hormone signaling can delay tumor growth progression, resistance develops over time when alternative signaling pathways are activated. The PI3K/AKT/mTOR pathway is one of the survival mechanisms activated during antihormonal therapy. The Phosphatidylinositol 3-kinase (PI3K) and Akt signaling cascade is critical for mTOR activation which is a cell kinase and an intracellular prolocal protein in intracellular signaling cascades [2]. The mTOR signaling network controls cell survival, glycolysis, and the suppression of pro-apoptotic proteins. Aberrant signaling of the PI3K/AKT/mTOR pathway can be suppressed by mTOR kinase inhibitors such as everolimus [3]. However clinical investigations have shown everolimus as a single drug has only a minor inhibitory effect on the progression of endocrine resistant breast cancer tumors [4]. This limited impact is hypothesized to result from enhanced activation of Akt via a feedback loop caused by downstream mTOR inhibition [3]. Melatonin (N-acetyl-5-methoxytryptamine) is a hormone, primarily secreted by the pineal gland and other organs and tissues such as retina, bone marrow cells, and skin. It has a wide range of biological effects including anti-oxidation, anti-inflammation, and anti-tumor activities [5–9]. Moreover, it is considered as a pharmaceutical compound with different therapeutic activities [10]. Melatonin has been shown to decrease tumor growth and survival in studies investigating its effects on hormone receptor-positive breast cancer cells [11, 12]. Melatonin may enhance the anti-proliferative effects of everolimus by inhibiting excess Akt production, induction pro-apoptotic pathways and disrupting tumor cell mitochondrial activities. However, the combined effects of melatonin and mTOR inhibition in hormone receptor-positive breast cancer cells remain underexplored.

The purpose of this work was to investigate the combined anti-cancer activity of melatonin and everolimus on the PI3K/AKT/mTOR pathway in MCF-7 (HR+, HER2-) breast cancer cell line, as well as the impact of these effects on mitochondrial energy pathways.

Materials and methods

Reagents, chemicals and antibodies

The following antibodies were obtained from trading sources; anti-p-4E-BP1 (1:750, Cell signaling, 2855), anti-p-p70S6K (Thr389) (1:750, Cell signaling, 9234),

anti-p-p70S6K (Ser371) (1:750, Cell signaling, 9208), anti-mTOR (1:750, Cell signaling, 2983), anti-p-mTOR (1:750, Cell signaling, 5536), anti-β-actin (1:1000,novus, NB600-501), anti-p62 (1:500, Abnova, H00008878-M01), anti-LC3-II (1:500, Cell signaling, 2775 S), anti-rabbit-Alexa 568 (Thermo), anti-mouse and anti-rabbit secondary antibodies (1:2000, Santa cruz, sc-2005-sc2004). Everolimus was purchased from Selleckchem, cell culture medium and additives were supplied from Gibco, melatonin and all other reagents were obtained from Sigma- Aldrich.

Cell culture and conditions

MCF-7 (HTB-22) breast cancer cell line was purchased from ATCC and grown in Dulbecco's Modified Eagle's Medium (DMEM). The media was supplemented with 10% fetal bovine serum (FBS), 2mM L-glutamine and 100 units/mL penicillin, 100 µg/mL streptomycin. Cells were kept in a humidified environment (37 °C and 5% CO_2 in the air). Cells were passaged every two to three days per week (1:4 ratio). The cells were trypsinized with 0.25% trypsin-EDTA solution after being rinsed with phosphate buffered saline (PBS) once they had attained 80–90% confluency. A hemocytometer was used to count cells before seeding, trypan blue.

Cell viability assay

The cell viability assay was performed with MTT. Cells were seeded in 96-well plates (1×10^4 cells/well) and allowed to attach overnight (16 h). The cells were exposed to a wide range of everolimus and melatonin concentrations for 72 h. The cells were then incubated in the dark for 4 hours with a 5-mg/ml solution of 3-(4,5-Dimethylthiazol-2-yl)-2,5-diphenyltetrazolium bromide (MTT). Formazan formed in living cells was dissolved in DMSO and the solution's absorbance at 570 nm was measured with a microplate reader [13].

Scratch-wound healing assay

MCF-7 cells were plated in 24-well plate at 5×10^5 cells/well in DMEM medium. Cells were incubated in FBS-free medium for an additional 24 h. Following the removal of the medium, 1xPBS was added to the wells to wash the cells. 200 µl pipette tip was used to set the reference point in each well, and the wells were then drawn vertically from this position [14]. Following the completion of the scratching procedure, PBS was withdrawn and the cells were washed once with a medium containing 0.5% FBS to remove cell debris generated in the medium. Images of the scratches were captured at 0, 24, 48 and 72 h with Nikon inverted microscope at 100× magnification. Cell migration was quantitated using Fiji ImageJ (NIH).

Apoptosis assay

MCF-7 cells were adhered overnight and treated for 72 h with melatonin (3 mM), everolimus (30 nM), melatonin/everolimus (3 mM + 30 nM) or control media. After the session, cells were treated and stained with Annexin V-fluorescein isothiocyanate (FITC) and propidium iodide (PI) (Invitrogen) according to the manufacturer's protocol (e-bioscience, Annexin FITC Apoptosis Detection kit, BMS500FI-100). Apoptosis was measured by flow cytometry (Becton Dickinson) as the percentage of annexin-V-, and PI-positive events.

Cell cycle analysis

MCF-7 cells were treated for 72 h with melatonin (3 mM), everolimus (30 nM), melatonin/everolimus (3 mM + 30 nM) or control media. After treatment, the cells were trypsinized, centrifuged at 500xg for 5 min and then rinsed with PBS. After draining the supernatant, they were fixed on ice with ice-cold 66% Ethanol/PBS for overnight at 4ºC. After washing the fixed cells PBS, RNase A (20 µg/ml) was applied, followed by PI (1 mg/ml) to stain the cells for 30 min in the dark according to the manufacturer's protocol (Abcam, propidium iodide flow cytometry kit, ab139418). The stained cells were examined using BD analyzer.

Western blotting

Total proteins were obtained by lysing cells using RIPA lysis buffer with protease inhibitor cocktail (Sigma-Aldrich). Protein concentrations were determined using the Bio-Rad protein Assay (BioRad, Hercules, CA, U.S.). 50 µg of protein samples were onto 10% sodium dodecyl sulfate–polyacrylamide gel electrophoresis (SDS-PAGE) and transferred them to the polyvinylidene difluoride (PVDF) membrane under wet conditions. The PVDF membranes were incubated sequentially with 5% bovine serum albumin, primary and secondary antibodies. The related proteins on PVDF membranes were detected with the western ECL HRP substrate (Amersham, UK) luminescence [15]. With the aid of Image J, pictures were analyzed.

Mitochondrial membrane potential analysis (MMP)

MCF-7 cells were seeded at 2×10^5 cells/well in a 6-well plate and treated according to the experimental protocols as described above [16]. Then JC-1 dye (1 µm) was then added and incubated at 37 °C for 15 min. MMP depolarization was seen using a Nikon fluorescence microscope at the emission wavelengths of red (Ex: 525/50, Em: 597/58) and green (Ex: 470/40, Em: 534/55). Lower red to green fluorescence ratios suggested more mitochondrial depolarization and lower $\Delta\Psi m$.

Immunofluorescence staining

For 72 h, the cells were exposed to melatonin, everolimus, melatonin + everolimus, and control medium as described. The cells were then fixed in 4% paraformaldehyde (PFA) for 30 min at + 4ºC, followed by a 1xPBS wash. Following 30 min of permeabilization with %0.1 BSA+%0.1 saponin at + 4ºC for, the cells treated with LC3-II primary antibodies (1:200) overnight at + 4ºC [12]. Following three PBS washes, cells were incubated with the fluorescent secondary antibody for two hours in the dark (Alexa 568, Thermo). After washing the cells with 1XPBS, images were captured using a Nikon microscope.

Analysis of mitochondrial respiration in digitonin permeabilized cells

Using a Clark oxygen electrode (Hansatech Instruments, UK) and continuous stirring (60 rpm), the mitochondrial respiration of digitonin permeabilized cells was assessed polarographically, as previously described [15]. While 10mM succinate, 2 µM rotenone and 500 µl respiratory buffer were present in the reaction chamber, approximately 2×10^6 cells were addedinto the medium. Following permeabilization with 0.006% digitonin, ADP (0.2 mM) was addedfor the determination of state 3 respiration. 5 µM oligomycin was added to the medium to test State 4 respiration. Uncoupling of the respiratory chain from ATP synthesis was achieved by the addition of 100 mM FCCP, which abolishes the electrochemical gradient. For the analysis of respiration over complex IV, N,N,N',N'-tetramethyl-p-phenylenediamine (TMPD)/Ascorbate (0.2 mM/10 mM) was used as the substrate and after roughly 3 min of measurement, respiration was inhibited by adding 700 µM potassium cyanide (KCN) to the medium. The final respiratory rate was obtained by subtracting the KCN insensitive respiration rate.

Statical analysis

SPSS 24 was used for statistical analyses (SPSS Inc., Chicago). All statistical analyses were carried out, and the data was examined with one-way ANOVA. Each bar graph represents the mean ± SEM (standard error of the mean) of ≥ 3 independent experiments. Values of $p < 0.05$ were considered as significant.

Results

Melatonin and everolimus (MEL/EVE) co-administration reduced cell viability and migration

Different doses of melatonin (0–6 mM), everolimus (0-125 nM) and their combination were applied over 24, 48, 72 h to investigate cell viability using MCF-7 cells. When 2 mM and 4 mM melatonin were applied alone, cell viability decreased by 28.85% and 47.1%, respectively ($p < 0.05$) after 72 h. (Fig. 1A). In 72 h, everolimus administration alone resulted in 29.87% cell death at a dosage of 31.25 nM. (Fig. 1A). When 31.25 nM everolimus was combined with 2 mM and 4 mM melatonin, cell viability at 72 h was, respectively, 62.60% and 42.58% (Fig. 1B). This rate is 70.13% after 72 h of treatment of 31.25 nM everolimus alone. Melatonin's 50% inhibitory concentration (IC50) was determined to be 3.21 M after 72 h. It was then followed by 3 mM melatonin and 30 nM everolimus concentrations.

Scratch assays on MCF-7 cells were conducted to further explore the effects of melatonin, everolimus, and MEL/EVE on cell migration. Cells were treated 24, 48, and 72 h with 3 mM melatonin, 30 nM everolimus, and MEL/EVE. The addition of drugs, either alone or in combination, resulted in a slower rate of wound closure compared to the control group over time. (Fig. 1C). As a consequence, the control group had 92% closure but rates for melatonin, everolimus, and MEL/EVE were 58%, 62%, and 37%, respectively (Fig. 1C). These data indicate that the co-administration of MEL/EVE significantly reduces the rate of wound closure compared to melatonin or everolimus alone.

MEL/EVE treatment inhibits growth of breast cancer cells via mTOR signaling pathways

The enhanced inhibition of breast cancer following of MEL/EVE administration, changes in mTOR signaling pathway in MCF-7 cells were examined. Protein levels of p-4E-BP1, p-p70S6K^{Ser371}, p-p70S6K^{Thr389}, mTOR, and p-mTOR were significantly lower after 72 h MEL/EVE treatment compared to the control group (Fig. 2A). While melatonin and everolimus reduced p70S6K-^{Ser371} expression by 0.1 and 0.16 fold, respectively, this ratio was 0.9 in contrast to the control following MEL/EVE treatment (Fig. 2B). Similarly, MEL/EVE application reduced p-p70S6K^{Thr389} protein expression (Fig. 2B). Interestingly, the p-4E-BP1 level was enhanced by melatonin and everolimus administration alone, but lowered by MEL/EVE administration (Fig. 2B). When mTOR and p-mTOR protein expressions were analyzed, MEL/EVE treatment resulted in a reduction in protein expression relative to control group and melatonin, while no significant change was observed in comparison to everolimus. Melatonin enhanced the impact of everolimus, a known mTOR inhibitor, on p-4E-BP1, p70S6K^{Ser371}, and p-p70S6K^{Thr389} protein expressions and significantly reduced protein levels.

MEL/EVE treatment promotes apoptosis and the accumulation of Sub-G1 in HR+, HER2- breast cancer cells

Next, we investigated the effects of melatonin and everolimus either alone or in their combination on apoptosis using flow cytometry with Annexin V/FITC-PI labelling method on MCF-7 cells (Fig. 3A). Apoptosis was significantly elevated ($p < 0.05$) after melatonin treatment alone.

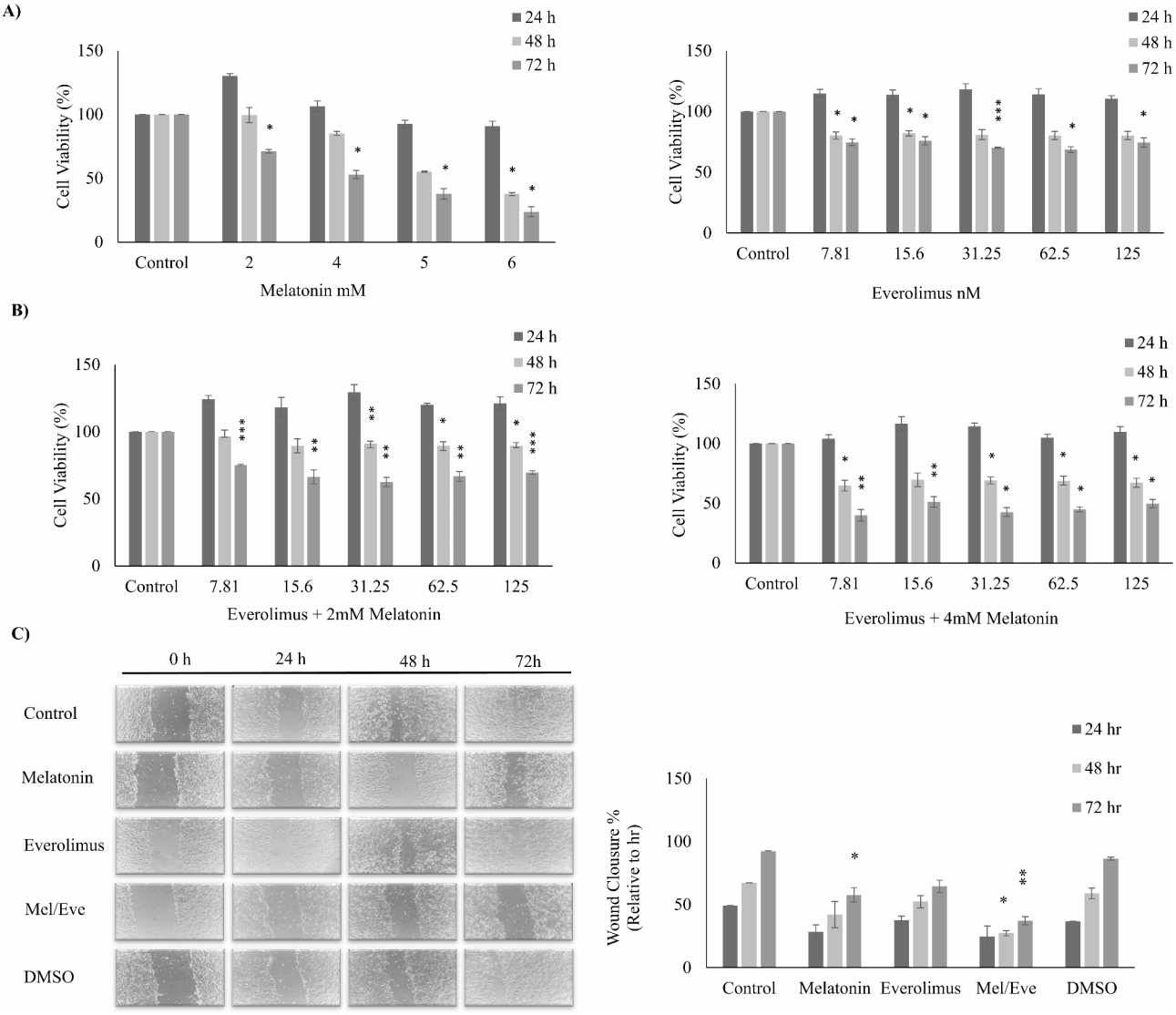

Fig. 1 Melatonin and everolimus combined therapy decreases MCF-7 proliferation. (**A**) MCF-7 cells were treated over 24, 48, 72 h with melatonin (2, 4, 5, 6 mM), everolimus (7.81, 15.6, 31.25, 62.5, 125 nM), and cell viability was assessed. (**B**) Cell viability in MCF-7 cells was investigated by combining 4 mM and 2 mM melatonin with varying dosages of everolimus for 24, 48, and 72 h. Normalized results for cell viability assays were represented as a percentage of the control. The data come from three separate trials. (**C**) Cell scratch assays were performed at 0, 24, 48, and 72 h in the treatments containing the control, melatonin (3 mM), everolimus (30 nM), and the combination of melatonin and everolimus. DMSO serves as a negative control. The amount of gap closing caused by the cells was measured and displayed as bar graphs. (Three separate tests were conducted). The bars represent mean ± SEM. *$p < 0.05$, **$p < 0.005$, ***$p < 0.0005$

Early, late, and overall apoptosis rates were found to be 6.55%, 1.87% and 8.42%, respectively, as compared to the control group. There was a reduction in late apoptosis ($p < 0.05$) when everolimus was used alone, but there was no a significant rise in early or overall apoptosis rates. Considering the MEL/EVE application, the rates of early, late and overall apoptosis were significantly increased, respectively, by 14.24% ($p < 0.0005$), 2.63% ($p < 0.05$) and 16.87% ($p < 0.0005$) (Fig. 3A). The overall apoptosis rate is 45.25% as a result of the administration of staurosporine, which is known to promote apoptosis in cells, (Data not shown). Melatonin significantly enhanced the efficacy of everolimus in MCF-7 cells and elevated the levels of apoptotic cell death.

We used PI staining and flow cytometry to explore the effect of melatonin, everolimus, and co-treatment with MEL/EVE over 72 h on cell cycle progression in MCF-7 cells (Fig. 3B). The proportion of G1 cells in the group given 3 mM melatonin was 69.9%, a substantial increase compare the control. In comparison to the control group, there was no significant difference in the G1 ratio of cells treated with everolimus alone or MEL/EVE combination (54.4% and 54.3%, respectively) ($p > 0.05$). While there was no significant difference in any group in the S

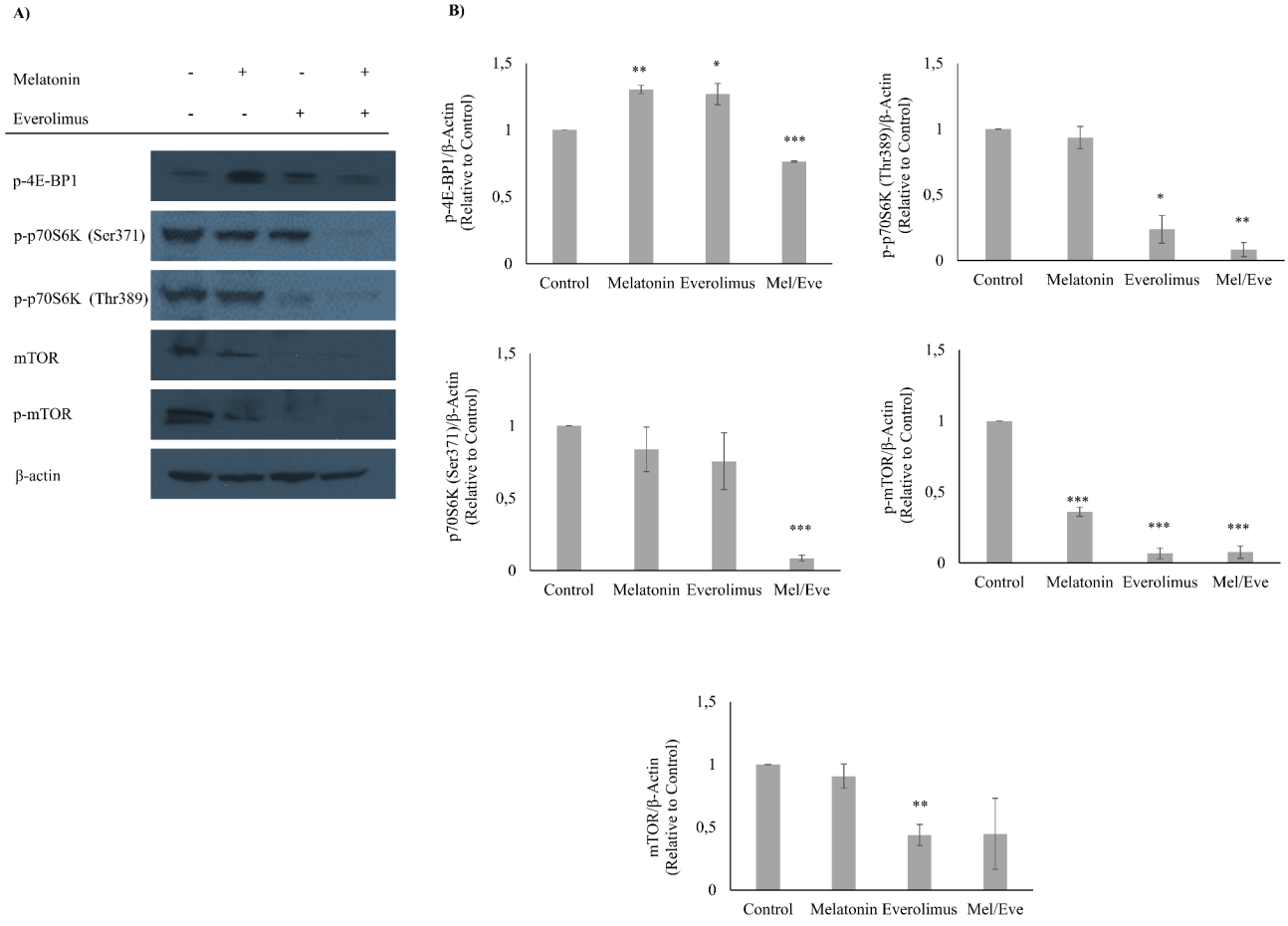

Fig. 2 MEL/EVE suppresses breast cancer cell proliferation via mTOR signaling pathways. (**A**) The mTOR pathway protein expression levels were evaluated after 72 h of treatment with melatonin, everolimus, and the MEL/EVE combination on MCF-7 cells. (**B**) Protein band quantitative analyses were performed and displayed as bar graphs. (At least three separate tests were carried out). The bars represent mean ± SEM. *$p < 0.05$, **$p < 0.005$, ***$p < 0.0005$

phase ($p > 0.05$). There was a significant reduction in cell accumulation in the G2 phase in the groups treated with melatonin (12.55%) and MEL/EVE (20.03%) compared to the control (29.51%) ($p < 0.005$) (Fig. 3B). Interestingly, G1 cell accumulation was significantly increased in the MEL/EVE treated group in our 48-hour data (Data not shown). The reduction in the number of cells in the G1 accumulation after 72 h, on the other hand, indicated that this accumulation was temporary. Furthermore, Sub-G1 cell accumulation was significantly increased in the MEL/EVE group compared to the control group and was 12.23%. This rate was statistically insignificant with the use of melatonin (2.47%) or everolimus (2.40%) alone. This result further supports a mechanism whereby melatonin induces cell growth suppression through the induction of apoptosis.

Melatonin and everolimus co-treatment increase autophagy activation in MCF-7 cells

Light chain 3 (LC3), a microtubule-associated protein present in autophagosomes, has been considered as an indication of autophagy. Using western blotting, we investigated autophagy flux in the MCF-7 cells by measuring changes in LC3-I and LC3-II levels, as well as the protein expression of SQSTM1/p62, which is known to become sequestered and degraded during autophagy. Melatonin, everolimus and MEL/EVE were also have impacts on LC3-II and p62 expression (Fig. 4A). In Fig. 4A also shows that p62 levels fell across all treatments and that sequestration occurred. As the band data were quantified, there was no significant increase in any of the groups when compared to the control, despite the fact that there was a conversion from LC3-I to LC3-II.

Hydroxychloroquine, which inhibits the vacuolar H + ATPase and inhibits autophagosome-lysosome fusion, was used to evaluate the dynamic process of autophagy in order to determine whether treatment groups increased the autophagosome formation or inhibited autophagy breakdown. Looking at the HCQ applied band data, there was no significant change in the transition from LC3-I to LC3-II in those treated with melatonin and everolimus. However, in the MEL/EVE group,

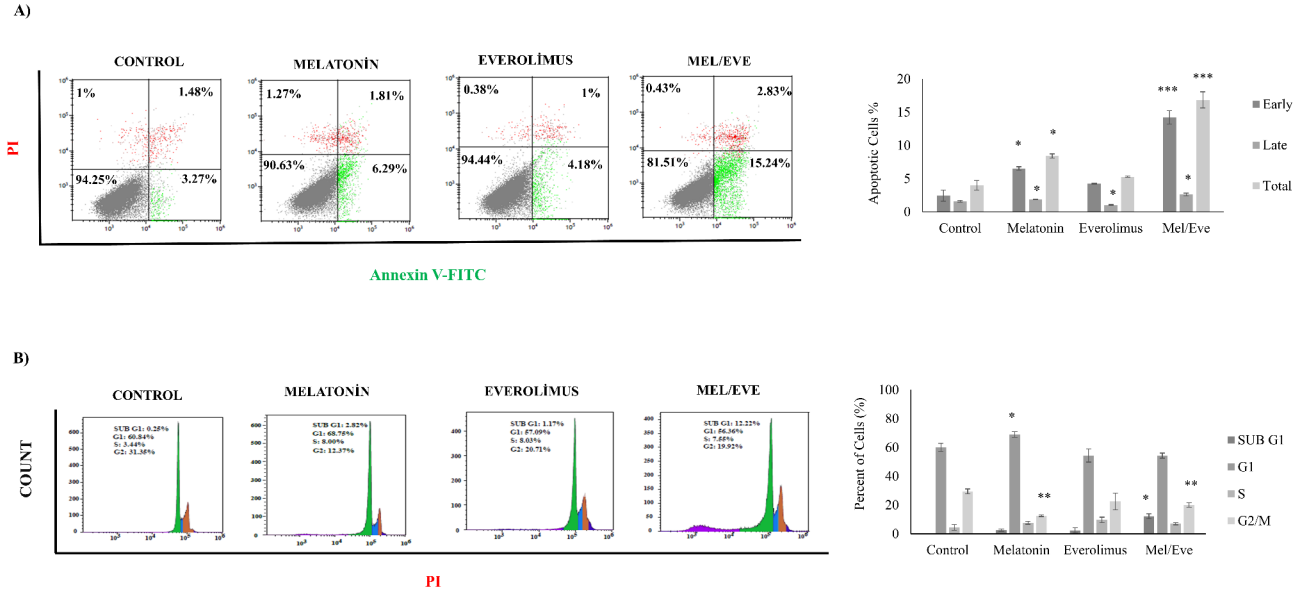

Fig. 3 MEL/EVE therapies cause apoptosis and the accumulation of sub G1 cells in HR+, HER2- breast cancer cells. **A** The amount of apoptosis was measured using annexin V-FITC labeling to detect apoptotic cells in comparison to untreated cells (control), followed by flow cytometry analysis. Bar graphs depict the apoptosis rate of each group.**B** Flow cytometry was used to examine the cell cycle distribution of 72-hour melatonin, everolimus, and MEL/EVE-treated MCF-7 cells. Bar graphs depict the cell cycle distribution rate of each group. (Three independent experiments were performed). The bars represent mean ± SEM. *$p < 0.05$, **$p < 0.005$, ***$p < 0.0005$

the LC3II/LC3-I ratio increased significantly (Fig. 4A). These results indicate that MEL/EVE treatment induces autophagosome formation.

Although p62 degradation and the conversion of LC3-I to LC3-II are indications of autophagy, the punctate location of autophagosomes was studied using immunofluorescence detection of the LC3-II to reveal active autophagy. Figure 4B shows that LC3-II clusters significantly increased in groups treated with melatonin, everolimus, MEL/EVE and HCQ ($p < 0.05$). When compared to the control group, similar results were obtained in samples treated with melatonin, everolimus, MEL/EVE, and HCQ. These results also revealed that the MEL/EVE induced autophagy flux was complete.

MEL/EVE co-treatment improved the respiration control rate

We performed oxygraph respiration assays in permeabilized MCF-7 cells to evaluate if the MEL/EVE therapy affected bioenergetics. Respiration in digitonin-permeabilized cells was evaluated by supplying mitochondria with succinate, a substrate linked to complex-II. The ADP-induced (state 3) respiration rate was reduced when melatonin and everolimus was applied alone ($p < 0.05$) but there was no difference in the MEL/EVE treated group compared to the control ($p > 0.05$) (Fig. 5A). In contrast, no significant change in FCCP-induced (state 3u) maximum respiration was identified in the drug-treated groups compared to the control group (Fig. 5C). Similarly, in all treatment groups, oligomycin-inhibited (state 4o) respiration, an indicative of proton leak via the inner mitochondrial membrane, remained unaffected (Fig. 5B).

Melatonin and everolimus treatments reduced the complex-II dependent respiratory control ratio (RCR: state3/state4o) in digitonin-permeabilized cells ($p < 0.05$) (Fig. 5D). However, the RCR rate increased dramatically ($p < 0.005$) as a result of MEL/EVE application. Also respiration rate was measured in the presence of TMPD/Ascorbate in order to determine the complex IV dependent respiratory and no significant difference was found (Fig. 5E). In order to asses mitochondrial membrane potential, JC-1 fluorescent staining method was used and no significant difference was found between control and MEL/EVE co-treatment group (Fig. 5F and G). These findings show that co-administration of melatonin and everolimus does not induce proton leak and mitochondrial uncoupling, but rather causes restoration of everolimus induced respiratory inhibition.

Discussion

Everolimus (RAD001) is a sirolimus derivative with improved hydrophilicity that is used for the inhibition of mTOR and regulation of cellular activities including protein synthesis, lipid synthesis, mitochondrial biogenesis and function, cell cycle and autophagy. However, resistance to everolimus is a common feature in many in vitro models of breast cancer. It is known that MCF-7 cells are resistant to everolimus and the calculated IC50 value for everolimus in MCF-7s are > 100 nM [17]. Many studies

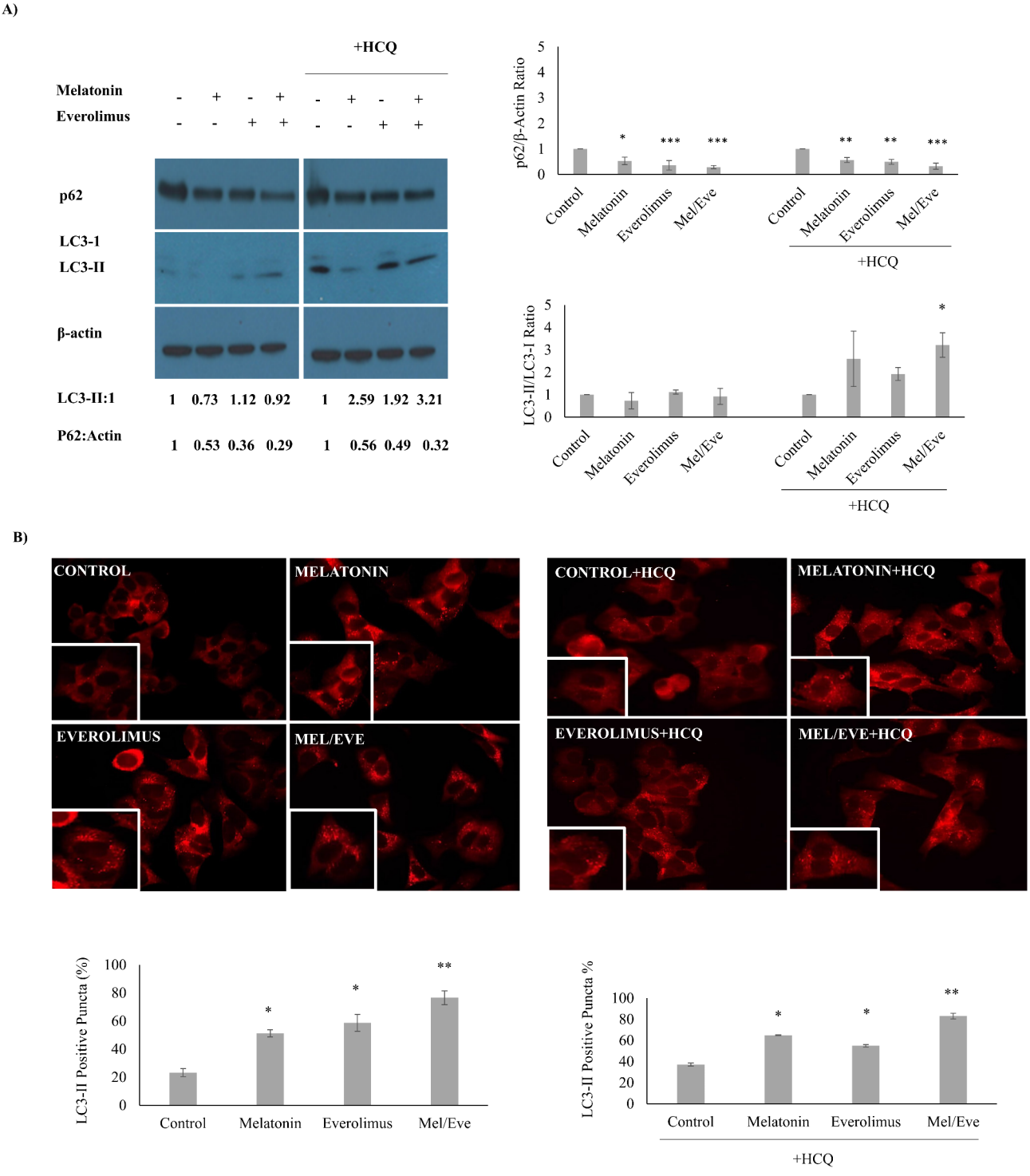

Fig. 4 Melatonin and everolimus co-treatment enhanced autophagy activation in MCF-7 cells. (**A**) Melatonin, everolimus, and MEL/EVE were administered to MCF-7 cells in the absence or presence of the lysosomal inhibitor hydroxychloroquine (HCQ, 10 M, 40 min), and the levels of p62, LC3-I, and LC3-II protein expression were measured. As a loading control, β-actin was employed. Protein band quantitative studies were carried out and displayed as bar graphs. (Three separate tests were carried out). ImageJ software was used to calculate band intensity ratios for the p62/Actin and LC3-II/LC3-I ratios. (**B**) Representative immunofluorescence images showing autophagosomal dot formation in MCF-7 cells labeled with LC3 was seen and quantified in the absence or presence of the lysosomal inhibitor HCQ, (10 M, 40 min). (At least four separate tests were carried out). The inset in the lower left corner represents a magnified view of a selected region from the main image, highlighting the structural details of LC3 puncta. The bars represent mean ± SEM. *$p < 0.05$, **$p < 0.005$

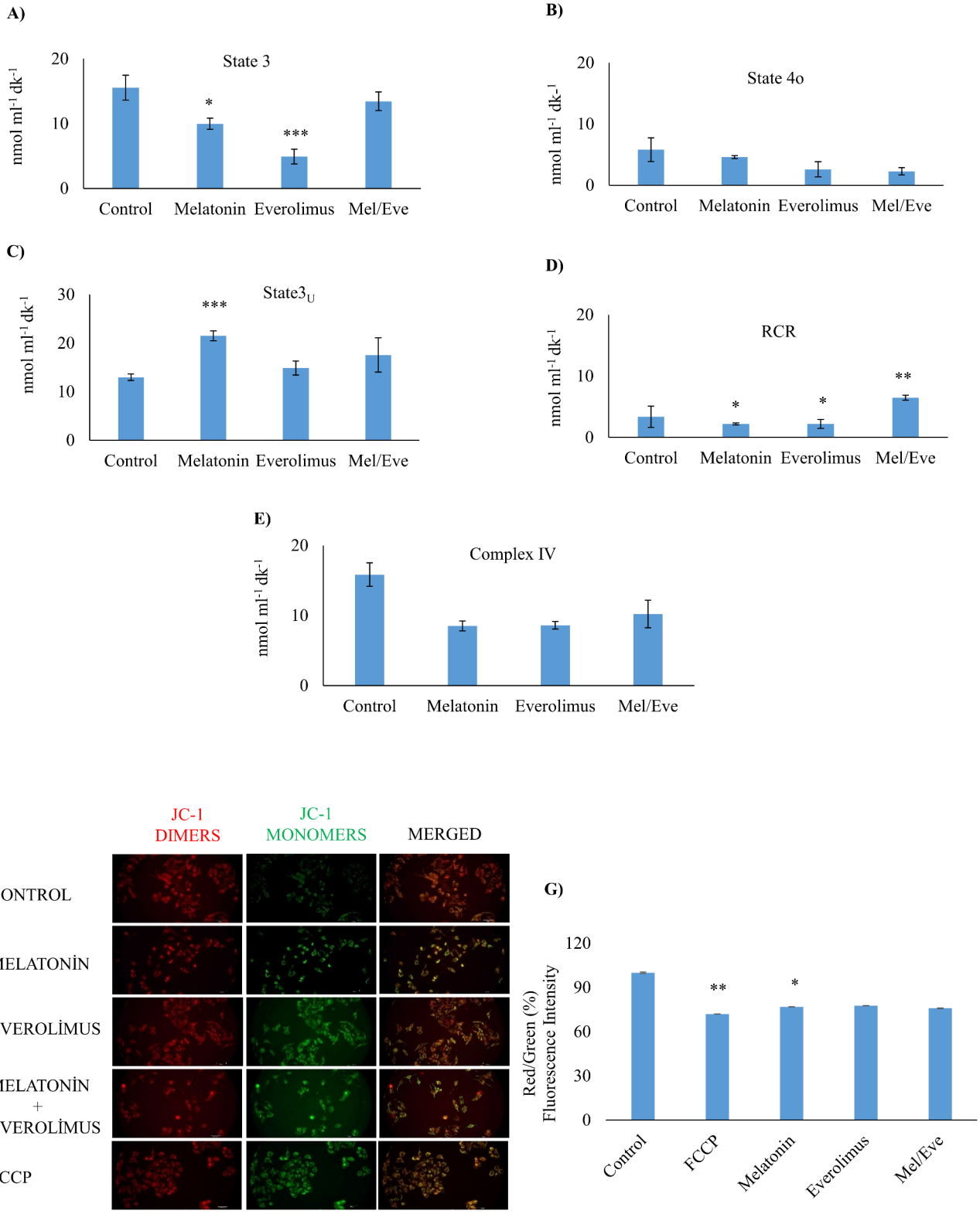

Fig. 5 (See legend on next page.)

(See figure on previous page.)

Fig. 5 Respiration rates in digitonin-permeabilized MCF-7 cells. MCF-7 cells supplied with succinate (10 mM) in the presence of 0.2 mM ADP (state 3) **A**, 5 µM oligomycin A (state 4o) **B**, 100 mM FCCP (State 3u) **C** and RCR calculation (state 3/state 4) **D** were examined by Hansatech Oxygraph. **E** OCR in digitonin-permeabilized MCF-7 cells with TMPD/ascorbate (0.2 mM/10 mM) was calculated Hansatech Oxygraph. (At least six independent experiments were performed). **F** Fluorescence pictures of cells labeled with JC-1 following treatment with the drugs in use (green damaged mitochondria, red healthy mitochondria). **G**. The amount of fluorescence intensity was measured with ımage J software and shown as bar graphs (At least ten independent experiments were performed). The bars represent mean ± SEM. *$p < 0.05$, **$p < 0.005$. OCR, oxygen consumption rate, RCR, respiratory control ratio; TMPD, N, N, N′, N′-tetramethyl-p-phenylenediamine

[18–22] have shown that melatonin administered as an adjuvant reduces cell viability and induces apoptosis. Here, we show that combining melatonin and everolimus improves effectiveness when compared to using everolimus alone.

Regarding the effects of melatonin and everolimus on cell viability, both melatonin and everolimus have been shown to inhibit cell viability and proliferation. However, co-administration of melatonin with everolimus caused a more dramatic decrease in cell viability and migration in MCF-7 cells. To date, no studies have been conducted to examine the combined effects of melatonin and everolimus on MCF-7 cell viability. Inhibition of mTOR and its downstream effectors the p70 ribosomal S6 kinases and eukaryotic translation initiation factor 4E binding protein 1 (4E-BP1) is one of the important targets in breast cancer treatment and cancer development. 4E-BP1 is a crucial biological component that modulates protein synthesis via the mTOR pathway. It is phosphorylated by mTORC1 [23]. Phosphorylation of 4E-BP1 prevents it from binding to eIF4E (eukaryotic translation initiation factor 4E) and activates a key mechanism that controls protein synthesis, leading to increased protein production in the cell. This promotes the survival and proliferation of cells. Inhibiting phosphorylation results in the binding of 4E-BP1 to eIF4E, which subsequently restricts protein synthesis. In cancers such as breast cancer, inhibiting the phosphorylation of 4E-BP1 can limit the overgrowth and survival of tumor cells [24]. In cancer treatment, this inhibition may be a critical target, as cancer cells are known to be associated with abnormal growth, proliferation, and excessive protein synthesis. Breast cancer is a heterogeneous disease with various molecular and environmental factors influencing its progression and treatment outcomes [25]. Understanding these factors is crucial for optimizing adjuvant therapeutic strategies. Our data indicate that the combination of melatonin and everolimus exerts a greater effect on inhibiting 4E-BP1 phosphorylation than either agent used independently.

p70S6 Kinase (p70S6K) is a serine/threonine kinase and is positioned downstream of the mTOR (mammalian target of rapamycin) signaling pathway. The mTOR/S6K pathway is activated in many malignancies owing to mutations, overexpression, or both of upstream positive regulators such as PI3K and Akt, or loss of expression and function of negative regulators such as the tumor suppressors PTEN and TSC1/2. The phosphorylation of Thr389 and Ser371 by mTORC1 is thought to be essential for canonical S6K1 activation [26]. The S6K isoform, S6K1, is crucial for cell growth, proliferation, and differentiation by modulating ribosome biogenesis, protein synthesis, cell cycle progression, and metabolism. The most well-defined locations are Thr229 (T229) in the activation loop and Thr389 (T389) within a conserved hydrophobic motif. Recent findings indicate that the Ser371 phosphorylation site is essential for Thr389 phosphorylation and S6K1 action [27]. Shin et al., demonstrated that GSK-3 positively regulates p70S6K activity by modifying Ser371 phosphorylation in HEK293 cells [28]. Melatonin had no effect on either amino acid residue's phosphorylation. This is consistent with previous studies [29, 30]. Furthermore, previous research has indicated that Ser371 phosphorylation is not rapamycin sensitive [28, 31] and Everolimus therapy had no effect on Ser371 phosphorylation. However, everolimus significantly reduced Thr389 phosphorylation, which is known to be rapamycin sensitive. In our study, phosphorylation of the Ser371 site was significantly decreased by the combined application of melatonin and everolimus. As a result of inhibition of Ser371 phosphorylation, inhibition of the p-Thr389 site was increased, and the mTOR downstream pathway-mediated cell viability and cell growth were obviously inhibited. Consequently, the regulation of the Ser371 site remains unknown. Cancer cells frequently exhibit an unregulated cell cycle, which promotes cell growth [32]. When the cell cycle stages are examined, only the melatonin-treated group experiences a G1 arrest. Melatonin and everolimus co-administration resulted in no cell cycle stoppage. Previous research has shown that combining everolimus with other drugs causes cell cycle arrest in the G0/G1 phase in MCF-7, BT474 and K562 cells [33, 34] as well as in the G2/M phase in MCF-7 cells when everolimus is combined with ribociclib [35]. However, in our study, it was observed that the increase in subG1 accumulation in the group where melatonin and everolimus were administered combined was approximately 12 times higher than in the control group. Sub G1 accumulation has been linked to apoptotic cell death. Based on this, when MCF-7s were stained with Annexin V-FITC/PI, the difference between early and late apoptosis increased dramatically when melatonin and everolimus were combined. Similarly, although melatonin treatment alone significantly raised

the incidence of both early and late apoptosis, everolimus administration alone specifically increased the rate of late apoptosis. These findings revealed that melatonin and everolimus co-administration promoted apoptotic cell death but had no effect on cell cycle arrest in 72-hour treatments.

Autophagy activation involves the conversion of LC3-I to LC3-II and the degradation of p62 [36]. We showed that co-administration of melatonin and everolimus caused p62 degradation but this co-administration only slightly altered the LC3-II/I ratio. Western analysis suggests that the number of repeats is insufficient. Furthermore, the LC3-II/LC3-I ratio increased as predicted in samples treated with HCQ, an autophagy inhibitor. LC3 clusters were also identified using fluorescence staining. Combined treatment with melatonin and everolimus increased the number of LC3 clusters. Furthermore, as predicted, the HCQ application has resulted in an increase in LC3 clusters. Melatonin increased the effectiveness of everolimus in activating autophagy in MCF-7 cells, according to these data.

Using suitable electron donor substrates and complex II and IV inhibitors, we investigated the effects of melatonin and everolimus co-administration on mitochondrial respiration. In complex II-mediated respiration, when melatonin and everolimus were delivered concurrently, the RCR rate increased compared to the control. Consequently, we have shown that the combination of melatonin and everolimus improves mitochondrial efficiency, which declines due to everolimus administration. There were no significant variations in complex IV-mediated respiration. In contrast to our findings, Lee et al. found that melatonin reduced maximal respiration and mitochondrial activity in Hep3B and Huh7 cells [37]. There are more studies that are comparable [38, 39]. It is believed that melatonin allows pyruvate to be converted to acetyl-CoA in the mitochondria, reprogramming glucose metabolism in cancer cells to a normal cell phenotype, which increases the rate of complex II-mediated mitochondrial RCR as a result of co-administration of melatonin and everolimus.

In conclusion, our results indicate that the co-administration of melatonin and everolimus increases the suppression of Ser371 phosphorylation of the S6K1 protein, which functions downstream in the mTOR pathway, in MCF-7 breast cancer cells. Thus, the inhibition of Thr389 phosphorylation is also enhanced. An increase in the suppression of 4E-BP1 phosphorylation has been observed. The suppression of phosphorylation of these two critical proteins involved in S6K function decreases cell growth and survival, while enhancing apoptosis and autophagic activation. In terms of mitochondrial function, co-administration of melatonin with everolimus did not cause proton leakage or mitochondrial uncoupling, but did restore everolimus-induced respiratory inhibition. This indicates that melatonin is a possible adjuvant, demonstrating its promising effects when combined with everolimus in breast cancer treatment. The mechanisms are summarized in Graphical Abstract.

Supplementary Information

The online version contains supplementary material available at https://doi.org/10.1186/s40360-025-00907-1.

Supplementary Material 1

Acknowledgements

Şeyma Demirkesen supported by TUBITAK-BIDEB 2211-A scholarship for Ph.D. studies.

Author contributions

Ş.D and C.A., designed the experiments. Ş.D., performed the experiments, image analyzed, prepared figures and designed graphical abstract. Ş.D., C.A., E.S.Ş., Y.İ., evaluated the results, wrote the manuscript and found financial support.

Funding

This work was supported by Scientific and Technological Research Council of Turkey (TUBITAK) 1002 grant number 222S127, Turkish Society of Medical Oncology (TTOD) grant number P-TTOD-2021-141 and Tekirdag Namık Kemal University BAP Project grant number: 1. DR. 22.355.

Data availability

The datasets generated and/or analyzed during the current study are available from the corresponding author on reasonable request.

Declarations

Ethical approval

The author of this article declares that the materials and methods used in this study do not require ethical committee permission and/or legal-special permissions.

Consent to participate

Not applicable.

Consent for publication

All authors give their consent for the publication of the data/manuscript.

Competing interests

The authors declare no competing interests.

Author details

[1]Department of Molecular Biology and Genetics, Faculty of Science and Arts, Namık Kemal University, Tekirdağ, Turkey
[2]Department of Medical Oncology, Balıkesir Ataturk City Hospital, University of Health Sciences, Balıkesir, Turkey
[3]Department of Medical Oncology, Faculty of Medicine, Tekirdağ Namık Kemal University, Tekirdağ, Turkey

Received: 2 December 2024 / Accepted: 17 March 2025
Published online: 12 May 2025

References

1. Howlader N, Cronin KA, Kurian AW, Andridge R. Differences in breast cancer survival by molecular subtypes in the united States. Cancer Epidemiol Biomarkers Prev. 2018;27(6):619–26.
2. Faivre S, Kroemer G, Raymond E. Current development of mTOR inhibitors as anticancer agents. Nat Rev Drug Discov. 2006;5(8):671–88.

3. Hay N. The Akt-mTOR Tango and its relevance to cancer. Cancer Cell. 2005;8(3):179–83.
4. Yardley DA, Noguchi S, Pritchard KI, Burris HA 3rd, Baselga J, Gnant M, et al. Everolimus plus exemestane in postmenopausal patients with HR(+) breast cancer: BOLERO-2 final progression-free survival analysis. Adv Ther. 2013;30(10):870–84.
5. Escames G, Leon J, Macias M, Khaldy H, Acuna-Castroviejo D. Melatonin counteracts lipopolysaccharide-induced expression and activity of mitochondrial nitric oxide synthase in rats. FASEB J. 2003;17(8):932–4.
6. Fernandez-Gil B, Moneim AE, Ortiz F, Shen YQ, Soto-Mercado V, Mendivil-Perez M, et al. Melatonin protects rats from radiotherapy-induced small intestine toxicity. PLoS ONE. 2017;12(4):e0174474.
7. Volt H, Garcia JA, Doerrier C, Diaz-Casado ME, Guerra-Librero A, Lopez LC, et al. Same molecule but different expression: aging and sepsis trigger NLRP3 inflammasome activation, a target of melatonin. J Pineal Res. 2016;60(2):193–205.
8. Doerrier C, García JA, Volt H, Díaz-Casado ME, Luna-Sánchez M, Fernández-Gil B, et al. Permeabilized myocardial fibers as model to detect mitochondrial dysfunction during sepsis and melatonin effects without disruption of mitochondrial network. Mitochondrion. 2016;27:56–63.
9. Calvo JR, Gonzalez-Yanes C, Maldonado MD. The role of melatonin in the cells of the innate immunity: a review. J Pineal Res. 2013;55(2):103–20.
10. Tordjman S, Chokron S, Delorme R, Charrier A, Bellissant E, Jaafari N, et al. Melatonin: pharmacology, functions and therapeutic benefits. Curr Neuropharmacol. 2017;15(3):434–43.
11. Blask DE, Sauer LA, Dauchy RT. Melatonin as a chronobiotic/anticancer agent: cellular, biochemical, and molecular mechanisms of action and their implications for circadian-based cancer therapy. Curr Top Med Chem. 2002;2(2):113–32.
12. Cos S, Sánchez-Barceló EJ. Melatonin and mammary pathological growth. Front Neuroendocr. 2000;21(2):133–70.
13. Unal O, Akkoc Y, Kocak M, Nalbat E, Dogan-Ekici AI, Yagci Acar H, Gozuacik D. Treatment of breast cancer with autophagy inhibitory MicroRNAs carried by AGO2-conjugated nanoparticles. J Nanobiotechnol. 2020;18(1):65.
14. Xu J, Liu D, Niu H, Zhu G, Xu Y, Ye D, et al. Resveratrol reverses doxorubicin resistance by inhibiting epithelial-mesenchymal transition (EMT) through modulating PTEN/Akt signaling pathway in gastric cancer. J Exp Clin Cancer Res. 2017;36(1):19.
15. Aral C, Demirkesen S, Bircan R, Yasar Sirin D. Melatonin reverses the oxidative stress and mitochondrial dysfunction caused by LETM1 Silencing. Cell Biol Int. 2020;44(3):795–807.
16. Sivandzade F, Bhalerao A, Cucullo L. Analysis of the mitochondrial membrane potential using the cationic JC-1 dye as a sensitive fluorescent probe. Bio Protoc. 2019;9(1).
17. Hurvitz SA, Kalous O, Conklin D, Desai AJ, Dering J, Anderson L, et al. In vitro activity of the mTOR inhibitor everolimus, in a large panel of breast cancer cell lines and analysis for predictors of response. Breast Cancer Res Treat. 2015;149(3):669–80.
18. Artemenko M, Zhong SSW, To SKY, Wong AST. p70 S6 kinase as a therapeutic target in cancers: more than just an mTOR effector. Cancer Lett. 2022;535:215593.
19. Chen YT, Yang CC, Shao PL, Huang CR, Yip HK. Melatonin-mediated downregulation of ZNF746 suppresses bladder tumorigenesis mainly through inhibiting the AKT-MMP-9 signaling pathway. J Pineal Res. 2019;66(1):e12536.
20. Cos S, Mediavilla MD, Fernández R, González-Lamuño D, Sánchez-Barceló EJ. Does melatonin induce apoptosis in MCF-7 human breast cancer cells in vitro? J Pineal Res. 2002;32(2):90–6.
21. Rubio S, Estevez F, Cabrera J, Reiter RJ, Loro J, Quintana J. Inhibition of proliferation and induction of apoptosis by melatonin in human myeloid HL-60 cells. J Pineal Res. 2007;42(2):131–8.
22. Tamura H, Kawamoto M, Sato S, Tamura I, Maekawa R, Taketani T et al. Long-term melatonin treatment delays ovarian aging. J Pineal Res. 2017;62(2).
23. Sridharan S, Basu A. Distinct roles of MTOR targets S6K1 and S6K2 in breast cancer. Int J Mol Sci. 2020;21(4):1199.
24. Lee BJ, Boyer JA, Burnett GL, Thottumkara AP, Tibrewal N, Wilson SL, et al. Selective inhibitors of mTORC1 activate 4EBP1 and suppress tumor growth. Nat Chem Biol. 2021;17(10):1065–74.
25. Rezaeean H, Kaydani GA, Saki N, Razmjoo S, Labibzadeh M, Yaghooti H. The IFN-γ + 874 A/T polymorphism is associated with malignant breast cancer in a population from the Southwest of Iran. BMC Res Notes. 2021;14(1).
26. Ma XM, Blenis J. Molecular mechanisms of mTOR-mediated translational control. Nat Rev Mol Cell Biol. 2009;10(5):307–18.
27. Saitoh M, Pullen N, Brennan P, Cantrell D, Dennis PB, Thomas G. Regulation of an activated S6 kinase 1 variant reveals a novel mammalian target of Rapamycin phosphorylation site. J Biol Chem. 2002;277(22):20104–12.
28. Shin S, Wolgamott L, Yu Y, Blenis J, Yoon SO. Glycogen synthase kinase (GSK)-3 promotes p70 ribosomal protein S6 kinase (p70S6K) activity and cell proliferation. Proc Natl Acad Sci U S A. 2011;108(47):E1204–13.
29. Ren M, Liu H, Jiang W, Zhou Z, Yao X, Liu Z, et al. Melatonin repairs osteoporotic bone defects in Iron-Overloaded rats through PI3K/AKT/GSK-3beta/P70S6k signaling pathway. Oxid Med Cell Longev. 2023;2023:7718155.
30. Shen YQ, Guerra-Librero A, Fernandez-Gil BI, Florido J, Garcia-Lopez S, Martinez-Ruiz L et al. Combination of melatonin and Rapamycin for head and neck cancer therapy: suppression of AKT/mTOR pathway activation, and activation of mitophagy and apoptosis via mitochondrial function regulation. J Pineal Res. 2018;64(3).
31. Romanelli A, Martin KA, Toker A, Blenis J. p70 S6 kinase is regulated by protein kinase Czeta and participates in a phosphoinositide 3-kinase-regulated signalling complex. Mol Cell Biol. 1999;19(4):2921–8.
32. Ansari N, Shahrabi S, Khosravi A, Shirzad R, Rezaeean H. Prognostic significance of CHEK2 mutation in progression of breast cancer. Lab Med. 2019;50(3):e36–41.
33. De Benedetti A, Graff JR. eIF-4E expression and its role in malignancies and metastases. Oncogene. 2004;23(18):3189–99.
34. Mamane Y, Petroulakis E, LeBacquer O, Sonenberg N. mTOR, translation initiation and cancer. Oncogene. 2006;25(48):6416–22.
35. Marinelli O, Romagnoli E, Maggi F, Nabissi M, Amantini C, Morelli MB, et al. Exploring treatment with ribociclib alone or in sequence/combination with everolimus in ER(+)HER2(-) Rb wild-type and knock-down in breast cancer cell lines. BMC Cancer. 2020;20(1):1119.
36. Kocaturk NM, Akkoc Y, Kig C, Bayraktar O, Gozuacik D, Kutlu O. Autophagy as a molecular target for cancer treatment. Eur J Pharm Sci. 2019;134:116–37.
37. Lee S, Byun JK, Kim NY, Jin J, Woo H, Choi YK, Park KG. Melatonin inhibits Glycolysis in hepatocellular carcinoma cells by downregulating mitochondrial respiration and mTORC1 activity. BMB Rep. 2022;55(9):459–64.
38. Ariaans G, Jalving M, Vries EG, Jong S. Anti-tumor effects of everolimus and Metformin are complementary and glucose-dependent in breast cancer cells. BMC Cancer. 2017;17(1):232.
39. Estaras M, Ortiz-Placin C, Castillejo-Rufo A, Fernandez-Bermejo M, Blanco G, Mateos JM, et al. Melatonin controls cell proliferation and modulates mitochondrial physiology in pancreatic stellate cells. J Physiol Biochem. 2023;79(1):235–49.

Publisher's note